Supplementary Table 1. Data collection, phasing and refinement statistics

	Complex ($Argos_{217}$-$Spitz_{EGF}$)		**NaBr MAD Complex**		**$Argos_{217}$**	**$Spitz_{EGF}$**
Data collection	APS (23IDD)				ALS (8.2.1)	APS (23IDD)
Space group	P1				C2	C2
Cell dimensions						
a, *b*, *c* (Å)	50.0, 51.3, 70.0				113.6, 64.3, 72.5	58.3, 36.2, 25.4
α, β, γ (º)	84.2, 74.8, 75.7				90, 101.6, 90	90, 103.1, 90
		Peak	*Inflection*	*Remote*		
Wavelength (Å)	0.97928	0.91961	0.91987	0.89312	0.9202	0.97928
Resolution (Å)	50-1.6 (1.66-1.6)	30-2.0 (2.06-2.0)	30-2.0 (2.06-2.0)	30-2.0 (2.06-2.0)	50-2.51 (2.58-2.51)	50-1.5 (1.55-1.5)
R_{merge}	0.065 (0.355)	0.069 (0.241)	0.061 (0.266)	0.065 (0.322)	0.055 (0.364)	0.047 (0.205)
I/σ	11.3(2.6)	13.2(4.4)	12.6(3.5)	11.5(2.4)	15.1(2.7)	16.3(4.6)
Completeness (%)	94.6(71.4)	97.8(92.7)	97.7(91.7)	95.1(77.4)	93.9(80.9)	91.6(56.6)
Redundancy	3.7(2.7)	3.8(3.3)	3.8(3.1)	3.7(2.7)	3.4(2.6)	5.3(3.6)
Refinement						
Resolution (Å)	40.8-1.6 (1.64-1.60)				35.5-2.51 (2.58-2.51)	30.5-1.50 (1.54-1.50)
No. unique reflections	75,593(4298)				15,720(1024)	7284(319)
R_{work}/ R_{free}	0.20/0.24 (0.26/0.31)				0.26/0.30 (0.34/0.39)	0.20/0.24 (0.27/0.34)
Model						
Protein	aa A97-144, 260-419; B97-144, 260-418 (Argos) aa C50-97; D50-97 (Spitz)				aa A98-144, 260-419 aa B100-144, 260-419	aa 48-97
#/ASU (atoms)	2(4088)				2 (3293)	1(406)
Br	18				-	-
Water	860				127	81
B-factors	25.7				44.6	20.7
Protein(Aos/Spi)	22.4(22/23)				44.6	18.3
Br	19.8				-	-
Water	41.2				65.3	33.2
R.m.s deviations						
Bond lengths (Å)	0.011				0.011	0.009
Bond angles (º)	1.35				1.20	1.16

Supplementary Results and Discussion **Nature 01-00681**

Structural basis for EGFR ligand sequestration by Argos

Daryl E. Klein, Steven E. Stayrook, Fumin Shi, Kartik Narayan, and Mark A. Lemmon

Department of Biochemistry and Biophysics, University of Pennsylvania School of Medicine, 809C Stellar-Chance Laboratories, 422 Curie Boulevard, Philadelphia, PA 19104-6059, U.S.A.

Intermolecular domain/domain interactions in $Argos_{217}$

Although domain 1 of Argos does not directly contact Spitz, it interacts with domains 2 and 3, and may position these two domains (the jaws of the C-clamp) ideally for their simultaneous interaction with a single Spitz molecule. In addition to being covalently linked, domain 1 makes several specific contacts with domain 2. Residues 119-121 in the domain 1 'thumb' make β sheet-like main-chain hydrogen bonds with strand β2 in the first domain 2 finger (Fig. S4a). Interestingly, we previously showed that mutating the conserved valine at position 121 reduces the Spitz-binding affinity of Argos, and impairs its function[1]. Additional interactions that stabilize the domain 1/2 relationship include hydrogen bonds between the side-chain of Q105 (from the domain 1 amino-terminus) and the main chain of the β2-strand in domain 2. The side-chain of D274 (in the tip of the second domain 1 finger) also hydrogen bonds with T324 (in the second finger of domain 2).

Extensive contacts are also seen between domains 1 and 3 of Argos in the complex (Fig. S4b). The tips of the domain 1 fingers touch the edge (strand β2) of the first domain 3 finger, and make several inter-domain hydrogen bonds. Notably, W132 (from finger 1 of domain1) interacts with a backbone carbonyl in the β2 strand of domain 3, and also contacts aliphatic side-chains in this region (including L371). R277 (from domain 1, finger 2) also contacts residues 374-375 in strand β2 of domain 3. Further domain 1/3 contacts include a salt bridge between the side-chains of E134 and R367, plus hydrogen bonds from Y128 and E129 in the tip of the first domain 1 finger to a pair of histidines (H391 and H392) in the domain 3 knuckle. Overall, interactions between these 2 non-contiguous domains buries ~1200 $Å^2$ of relatively polar (51% polar) surface, with a high surface complementarity (S_c = 0.77).

Conformational change in Argos upon $Spitz_{EGF}$ binding

A comparison of $Argos_{217}$ structures with- and without bound $Spitz_{EGF}$ reveals a large reorientation of domain 3 upon ligand binding (Fig. S5). Domains 1 and 2 remain fixed in the orientation shown in Fig. S4a, but domain 3 is rotated by ~90˚ about an axis in the domain 2/3 linker, and translates 7Å along this axis (Fig. S5). Intriguingly, this conformational change amounts to a 'closure' of the Argos C-clamp in the absence of Spitz. All of the domain 1/3 interactions seen in the complex (Fig. S4b) are lost, and domain 3 'collapses' against domain 2 so that the Spitz binding sites of domains 2 and 3 come into direct contact with one another (right-hand panel in Fig. S5). Comparison of the left-most and right-most panels in Fig. S5 shows that finger 2 of domain 3 replaces the Spitz B-loop on the domain 2 ligand-binding surface.

In the process of binding to unliganded $Argos_{217}$, $Spitz_{EGF}$ must wedge itself between domains 2 and 3, and separate them (proceeding from right to left in Fig. S5). To function as an effective ligand sink, Argos must bind tightly to Spitz – suggesting that the intramolecular

domain 2/3 contacts seen in Fig. S5 do not present a significant impediment to Spitz binding. Indeed, $Argos_{217}$ binds $Spitz_{EGF}$ with K_D = 8nM (Fig. S2), around 20-fold more strongly than Spitz or EGF binding to soluble EGFR extracellular regions[2,3]. The intramolecular domain 2/3 interface in unliganded $Argos_{217}$ has characteristics of a weak interaction, consistent with this expectation. Although an average of 590Å^2 (69% apolar) is buried on domains 2 and 3 in this intramolecular interaction (compared with an average of 700Å^2 buried by $Spitz_{EGF}$ in each domain), the surface complementarity (S_c) is very low (at just 0.48, compared with 0.70 in Argos/Spitz interfaces), suggesting that it is weak and poorly packed.

Unliganded $Argos_{217}$ crystallized as a symmetric dimer, although analytical ultracentrifugation experiments (not shown) reveal that dimerization is rather weak in solution ($K_D \geq 20\mu M$). The crystallographic dimer is stabilized largely by antiparallel association of the β2 strands of two molecules (from finger 1 of domain 3), allowing an 8-stranded β-sheet to continue across the dimer (Fig. S6). Formation of this dimer requires domain 3 to be in the orientation found in crystals of unliganded $Argos_{217}$ (Fig. S5, right-most panel), and domain 3 may be trapped in this position by dimerization in the crystal. Given the feeble interface between domains 2 and 3, it seems likely that the orientation of domain 3 will not be fixed in the $Argos_{217}$ monomer that predominates in solution at physiological concentrations. Spitz binding could then lock a mobile domain 3 into the position seen in the $Argos_{217}$/$Spitz_{EGF}$ complex (which is monomeric in solution[2]).

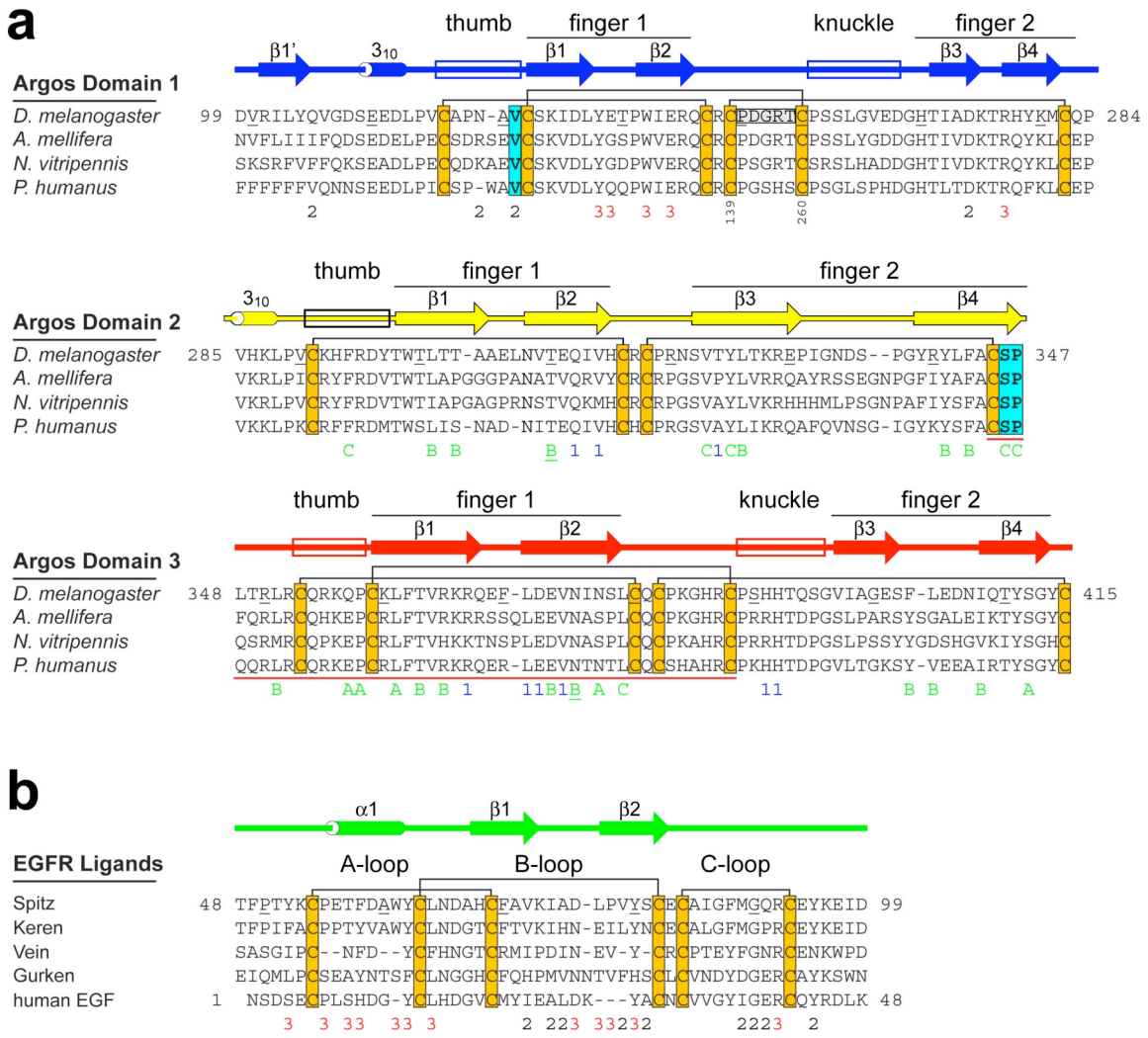

Figure S1

a, Argos sequences from *Drosophila melanogaster*, *Apis mellifera*, *Nasonia vitripennis* and *Pediculus humanus* are aligned and separated into the three constituent domains. Elements of secondary structure seen in $Argos_{217}$ are indicated above the sequence. In the *D. melanogaster* Argos sequence, every tenth residue is underlined. Positions of the thumb and knuckle loops are boxed (note that domain 2 has no knuckle). Disulphide connectivity is drawn with black lines between cysteines (orange boxes). The PDGRT linker used in $Argos_{217}$ to replace amino-acids 140-259 of intact *D. melanogaster* Argos is boxed grey. Sites at which mutations impaired Argos function in a genetic screen[1] (V121, S346, P347) are boxed with cyan. The initially proposed[4,5] EGF-like domain in Argos (primarily in domain 3) is underlined in red. Residues are marked beneath the alignment according to their inter- and intramolecular interactions. Residues that contact Spitz are labelled (in green) A, B, or C – depending on whether they contact the A-, B- or C-loop of Spitz (see **b**). Argos residues involved in intramolecular domain-domain contacts are numbered according to the domain with which they interact (1, 2 or 3). Two residues involved in both inter and intramolecular contacts (T310 and N375) are underlined. **b**, Alignment of the EGF domains from *D. melanogaster* EGF receptor-activating ligands and human EGF. Disulphides and secondary structure elements are marked as in **a**, and the positions of the A-, B- and C-loops are shown. Beneath the alignment, Spitz residues that contact Argos are labelled 2 (black) or 3 (red), according to the domain in Argos that each contacts.

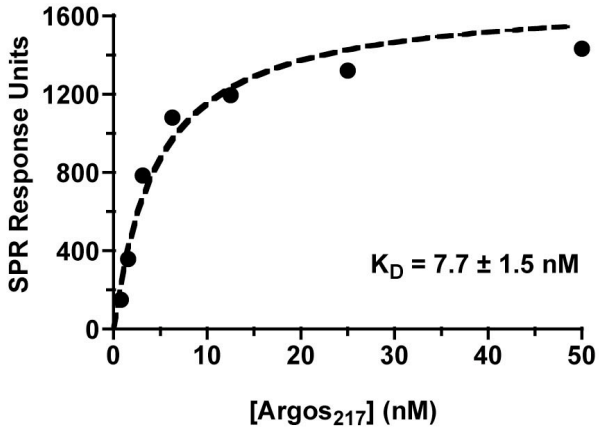

Figure S2 Binding of Argos$_{217}$ to Spitz$_{EGF}$

Representative surface plasmon resonance (SPR) binding curve for the interaction of soluble Argos$_{217}$ with immobilized Spitz$_{EGF}$. Experiments were performed exactly as described[2]. The mean K_D for Argos$_{217}$ binding to Spitz$_{EGF}$ (7.7±1.5nM) is comparable to values for binding of full-length secreted Argos$_{419}$ to intact secreted Spitz (20±3nM) or Spitz$_{EGF}$ (24±23nM)[2].

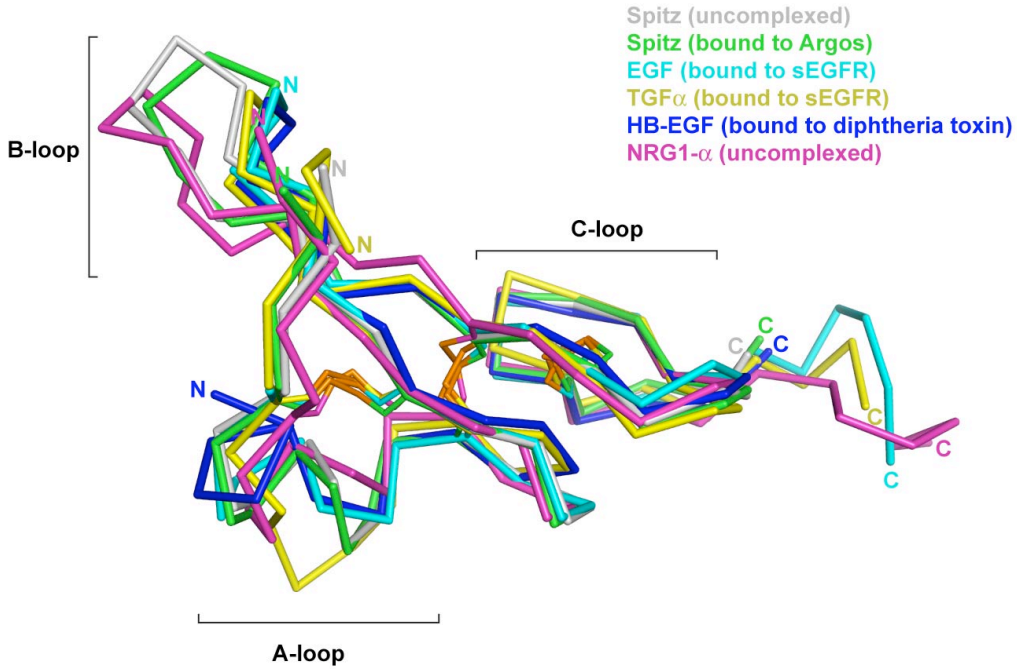

Figure S3 Overlays of EGF domain structures

Unbound (grey) and Argos-bound (green) Spitz are shown overlaid with crystallographically-derived (sEGFR-bound) structures of EGF[6] (cyan) and TGFα[7] (yellow), diphtheria toxin-bound HB-EGF[8] (blue/purple), and an NMR structure[9] of free NRG1-α (magenta). Note that Spitz most closely resembles NRGα in the length and approximate conformation at the end of the B-loop. The tip of the B-loop is also the only region in which clear differences between free (grey) and bound (green) Spitz can be discerned.

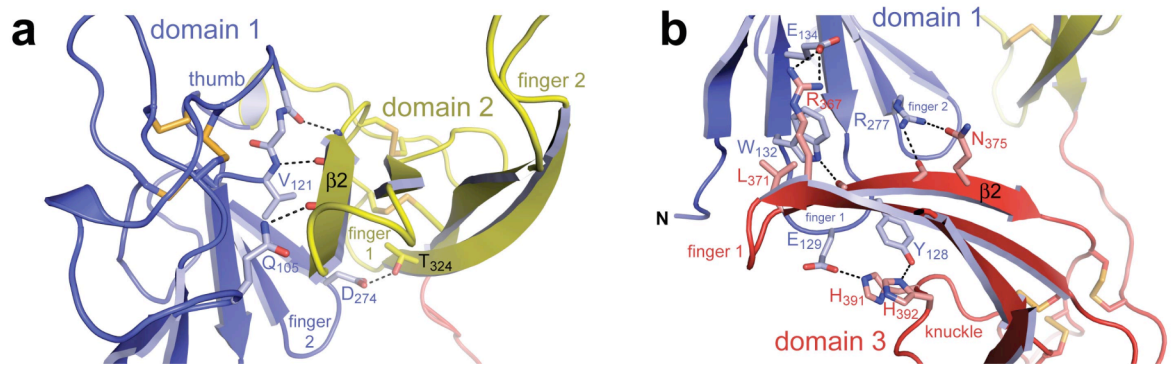

Figure S4 Interdomain interactions in Argos

a, Detail of interactions between Argos domains 1 (blue) and 2 (yellow) in the $Argos_{217}$–$Spitz_{EGF}$ complex. Domain 2 is in approximately the same orientation as in Fig. 1c in main text (left panel). These interactions are not altered by Spitz binding. **b**, Detail of interactions between Argos domain 1 (blue) and 3 (red) in the $Argos_{217}$–$Spitz_{EGF}$ complex. This set of interactions is only seen in the complex. Domains 1 and 3 do not make contact in unliganded Argos.

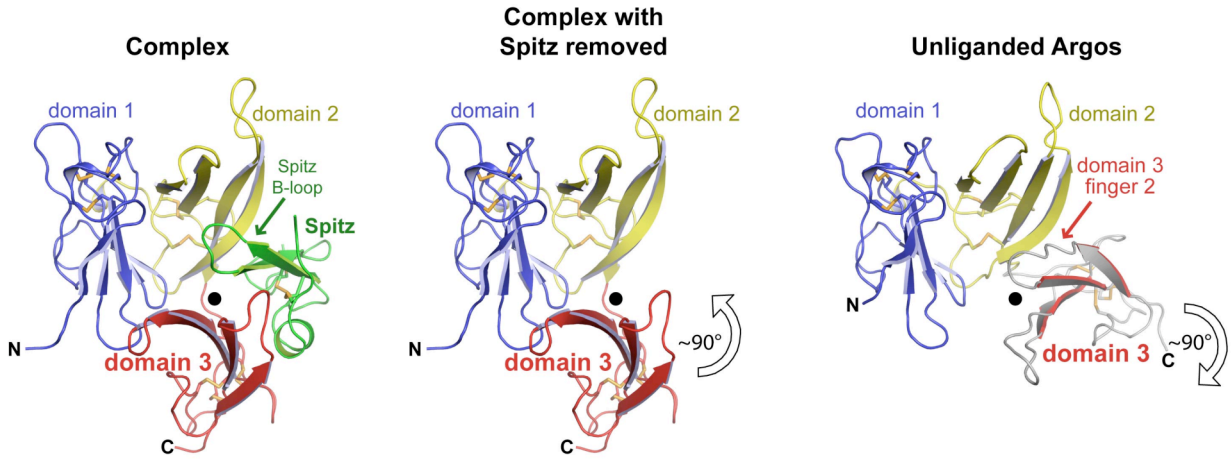

Figure S5 Conformational change in Argos upon binding to $Spitz_{EGF}$

$Spitz_{EGF}$ binding is associated with reorientation of domain 3. In the absence of bound Spitz, domain 3 of Argos undergoes a rotation of 90˚ about the axis marked with a black circle in the figure. In addition, domain 3 is translated 7Å into the page along this axis. This rotation breaks all domain 1/3 interactions seen in the Argos:Spitz complex (see Fig. S4b). Domain 3 effectively 'collapses' against the Spitz binding site on domain 2, and places its second finger where the Spitz B-loop lies in the complex.

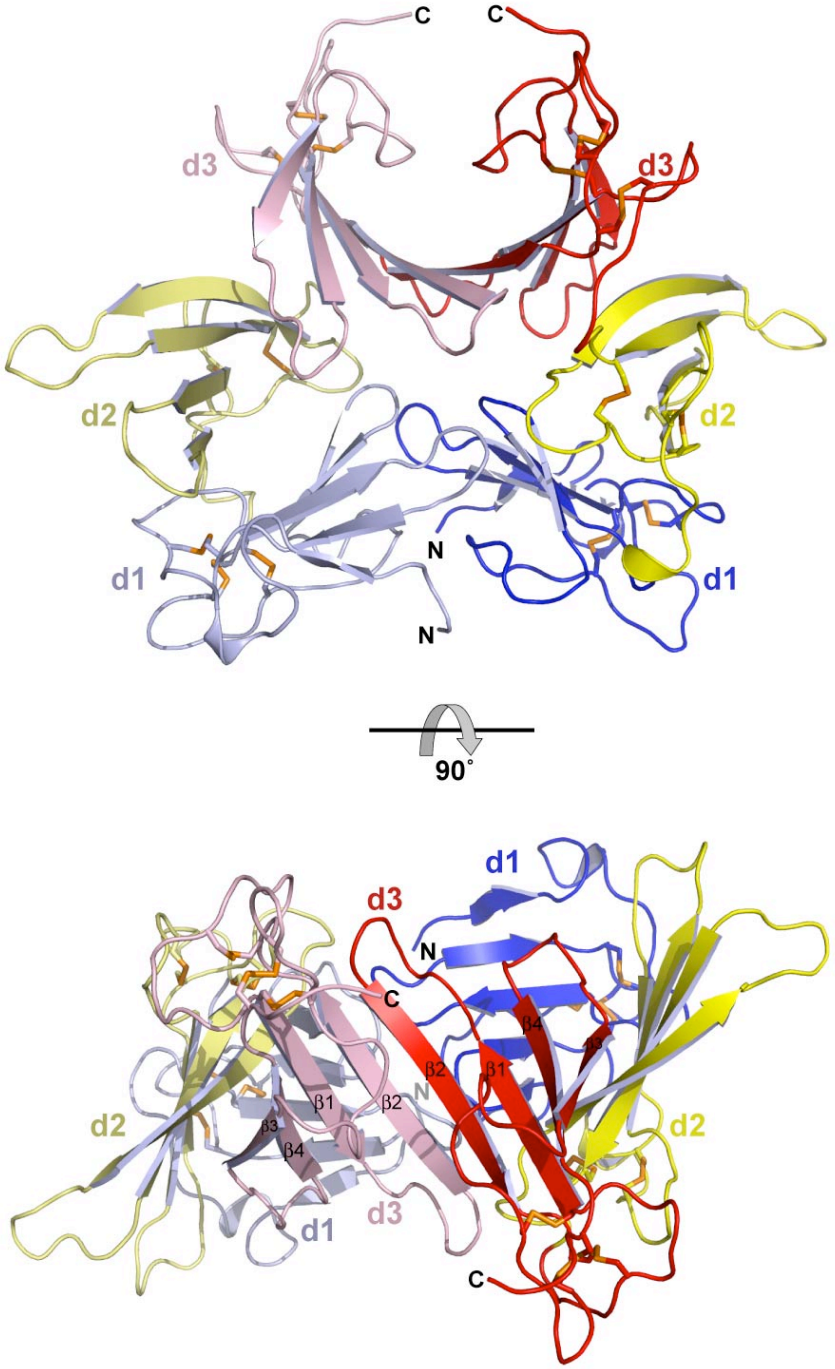

Figure S6 Dimer of unbound $Argos_{217}$ observed in crystals.

Two orthogonal views are shown for the dimer of $Argos_{217}$ seen in crystals that lack Spitz. Analytical ultracentrifugation studies indicate that this dimer can form in solution, but with a high K_D value of approximately 20μM. Dimerization is mediated primarily by backbone hydrogen bonding that extends the sheet formed by strands β1-β4 of domain 3 across two domains (and two molecules). As described in the text, the domain 3 reorientation that occurs upon Spitz binding prevents formation of this weak dimer.

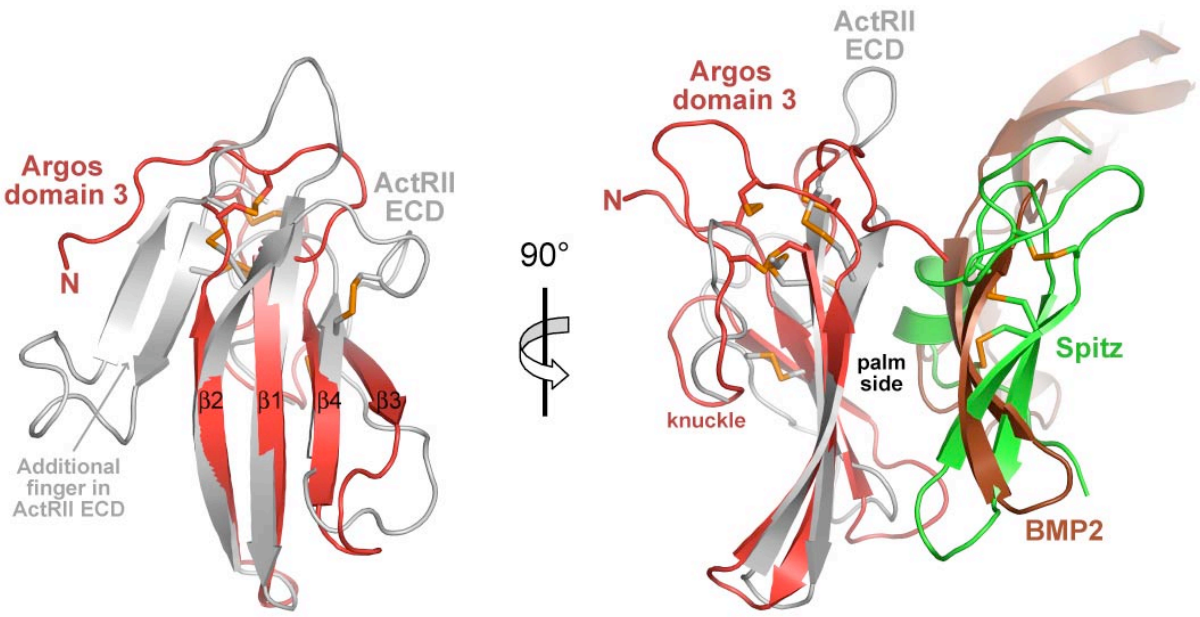

Figure S7 Similarity of Argos to TGFβ-family receptors

a, Domain 3 of Argos (red) is overlaid with the 100aa extracellular ligand-binding domain (ECD) of the type II activin receptor (ActRII)[10] (coloured light grey: from pdb entry 2GOO). The two fingers of each Argos domain overlay well with the longest fingers of the ActRII three-finger toxin fold. In addition, the disulphide-bonded cores are similarly located. The right-hand panel shows an orthogonal view in which Spitz and the receptor-proximal region of BMP2 (bound to ActRII) are shown. Both ligands bind to the palm side of their respective binding domains. The 'third' finger of the ActRII ECD has been removed from this view for clarity. The opposite end of the extended BMP2 molecule binds to a similar site on a type I receptor[10] (not shown).

References for Supplementary Material

1. Alvarado, D., Evans, T. A., Sharma, R., Lemmon, M. A., & Duffy, J. B. Argos mutants define an affinity threshold for spitz inhibition in vivo. *J. Biol. Chem.* **281,** 28993-29001 (2006).

2. Klein, D. E., Nappi, V. M., Reeves, G. T., Shvartsman, S. Y., & Lemmon, M. A. Argos inhibits epidermal growth factor receptor signalling by ligand sequestration. *Nature* **430,** 1040-1044 (2004).

3. Ferguson, K. M. *et al.* EGF activates its receptor by removing interactions that autoinhibit ectodomain dimerization. *Mol. Cell* **11,** 507-517 (2003).

4. Freeman, M., Klambt, C., Goodman, C. S., & Rubin, G. M. The argos gene encodes a diffusible factor that regulates cell fate decisions in the Drosophila eye. *Cell* **69,** 963-975 (1992).

5. Kretzschmar, D. *et al.* Giant lens, a gene involved in cell determination and axon guidance in the visual system of *Drosophila melanogaster*. *EMBO J.* **11,** 2531-2539 (1992).

6. Ogiso, H. *et al.* Crystal structure of the complex of human epidermal growth factor and receptor extracellular domains. *Cell* **110,** 775-787 (2002).

7. Garrett, T. P. J. *et al.* Crystal structure of a truncated epidermal growth factor receptor extracellular domain bound to transforming growth factor alpha. *Cell* **110,** 763-773 (2002).

8. Louie, G. V., Yang, W., Bowman, M. E., & Choe, S. Crystal structure of the complex of diphtheria toxin with an extracellular fragment of its receptor. *Mol. Cell* **1,** 67-78 (1997).

9. Jacobsen, N. E. *et al.* High-resolution solution structure of the EGF-like domain of heregulin-alpha. *Biochemistry* **35,** 3402-3417 (1996).

10. Allendorph, G. P., Vale, W. W., & Choe, S. Structure of the ternary signaling complex of a TGF-beta superfamily member. *Proc. Natl. Acad. Sci. U. S. A.* **103,** 7643-7648 (2006).